A Journal of the Gesellschaft Deutscher Chemiker

Angewandte International Edition GDCh Chemie

www.angewandte.org

Accepted Article

Title: Cellular AND Gates: Synergistic Recognition to Boost Selective Uptake of Polymeric Nanoassemblies

Authors: Jingjing Gao, Peidong Wu, Ann Fernandez, Jiaming Zhuang, and Sankaran Thayumanavan

To be cited as: *Angew. Chem. Int. Ed.* 10.1002/anie.202002748
Angew. Chem. 10.1002/ange.202002748

Link to VoR: http://dx.doi.org/10.1002/anie.202002748
http://dx.doi.org/10.1002/ange.202002748

WILEY-VCH

10.1002/anie.202002748

WILEY-VCH

COMMUNICATION

Cellular AND Gates: Synergistic Recognition to Boost Selective Uptake of Polymeric Nanoassemblies

Jingjing Gao[a], Peidong Wu[a], Ann Fernandez[a], Jiaming Zhuang*[a], S. Thayumanavan*[a][b][c]

[a] J. Gao, P. Wu, A. Fernandez, Dr. J. Zhuang, Prof. Dr. S. Thayumanavan, Department of Chemistry
[b] Molecular and Cellular Biology Program
[c] Center for Bioactive Delivery
University of Massachusetts Amherst, Amherst, MA 01003 (USA)
Email: jzhuang@chem.umass.edu; thai@chem.umass.edu
Supporting information for this article is given via a link at the end of the document.

Abstract: Development of nanoparticle based biomedical applications has been hampered due to undesired off-target effects. Here we outline a set of cellular AND gate concepts to enhance selectivity, where a nanoassembly-cell interaction is turned on, only in the concurrent presence of a two different protein functions, an enzymatic reaction (ALP) and a ligand-protein (CA IX) binding event. Selective uptake of nanoassemblies was observed in cells that overexpress both of these proteins (unicellular AND gate). Interestingly, selective uptake can also be achieved in CA IX overexpressed cells, when cocultured with ALP overexpressed cells, where the nanoassembly presumably acts as a mediator for cell-cell communication (bicellular AND gate). Demonstration of these logic-gated cellular uptake will find use in applications such as tumor imaging or theranostics.

Biological systems rely on cellular communications to generate precise responses, where cell surface receptors and enzymes are major conduits.[1] Similarly, cell surface proteins are the primary handles in targeting therapeutic molecules and imaging modalities in many diseases, such as in immunotherapy and in classifying cancer types.[2] Despite identifying cell surface target proteins, efforts towards specific on-target accumulation have resulted in minimal success.[3] Because, although active targeting relies on the incorporation of ligands on nanoparticles to recognize receptors overexpressed on tumor cell surfaces,[4] presence of low level of receptors in off-target locations can still hamper the specificity of these ligand-decorated nanocarriers. Nature often overcomes these specificity issues through Boolean logic, where the need for the concurrent presence of two different signals are imposed for a process to occur, an AND gate.[5] Inspired by this capability, we sought out to designing a cellular AND gate, where two different signals must be present in a single cell for the cell to efficiently take up a polymer nanoassembly – unicellular AND gate.

Additionally, biological systems also use cell-cell communications to execute many functions.[6] With logic-based polymeric assemblies as the tool, we were interested in also designing systems, where the processing of the nanoassembly by a specific protein in one cell activates it for a different cell with a complementary surface signature – a bicellular AND gate.

To test this possibility, we chose alkaline phosphatase (ALP) and carbonic anhydrase IX (CA IX) as the two cell surface proteins, as both of these are known to be overexpressed on certain pathological cells.[7] Our design strategy for this purpose is shown in Figure 1. Here, the ligand moiety for CA IX protein is incorporated onto a polymeric nanoassembly, but it is masked with another functionality, making it unavailable for binding to the cell surface protein. We envisaged designing the masking functionality such that it will be removed upon reaction with ALP. With this design, the nanoassembly would require the concurrent presence of both CA IX and ALP for activated uptake by cells (Figure 1).

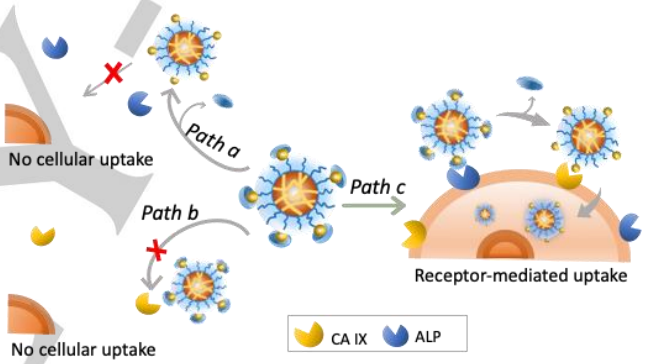

Figure 1. Schematic representation of cellular AND gated nanoparticle uptake. Path a: ligand on the surface of the nanoassembly is unmasked by the enzyme, but no active cellular uptake due to the absence of the complementary protein. Path b: the ligand is not unmasked due to the absence of the unmasking enzyme and is not available for active cellular uptake despite the presence of complementary protein; Path c: the presence of both the unmasking enzyme and the complementary protein causes receptor-mediated cellular uptake.

The molecular design strategy for the polymer assembly is shown in Scheme 1. We designed an amphiphilic diblock copolymer (Mn= 8.8 K Da, Đ= 1.02.), containing polyethylene glycol (Mn = 5 K Da) as the hydrophilic block and a coumarin-bearing alkylmethacrylate as the hydrophobic block. The critical cell-surface recognizing functionality was incorporated at the hydrophilic terminus, as this part of the polymer would be solvent-exposed and available for binding, when assembled in aqueous phase. We chose aryl sulfonamide as the ligand for binding CA IX. The key ligand-protein binding interaction here is based on the sulfonamide moiety binding to the zinc ion in the active site of the CA IX protein.[8] Therefore, we use the sulfonamide moiety to introduce a masking group, as this would both functionally and sterically make the aryl sulfonamide moiety unavailable for the protein. Thus the sulfonamide moiety was protected with p-substituted benzyl carbamate, as shown in Scheme 1. The substitution at the para-position is based on a phosphate moiety. Here, the ALP-induced cleavage of the phosphate moiety would liberate the p-phenolic functionality

10.1002/anie.202002748
WILEY-VCH

COMMUNICATION

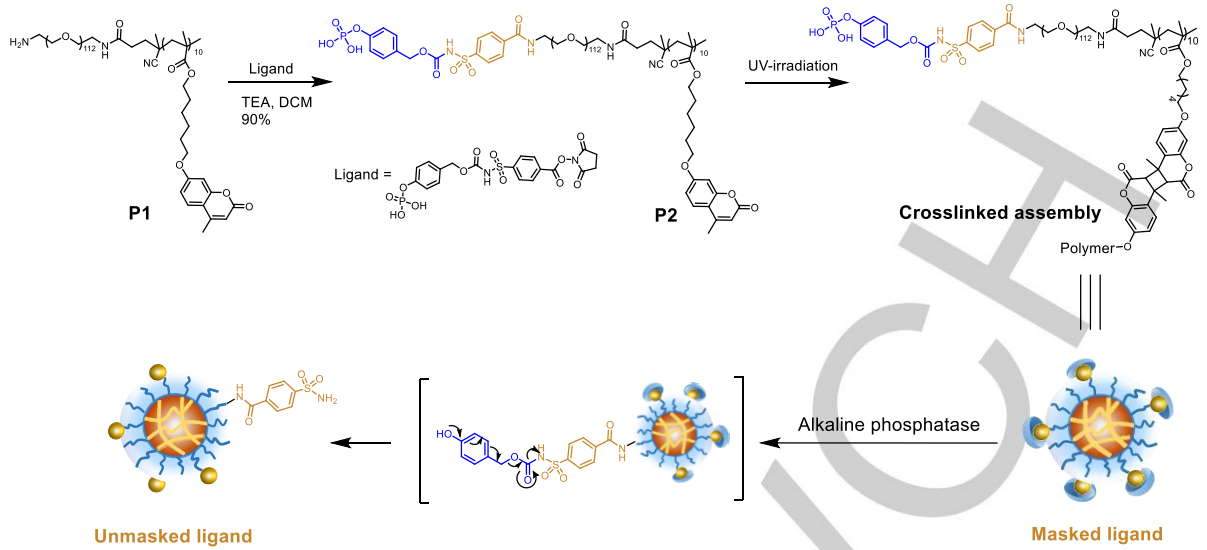

Scheme 1. Polymer synthesis route and ALP induced exposure of sulfonamide ligands.

which would undergo a cascade reaction to reveal the sulfonamide moiety. The synthetic approach to this polymer is shown in Scheme 1.

The amphiphilic nature of diblock copolymer P2 resulted in the formation of a nanoassembly in aqueous phase, with an apparent hydrodynamic diameter of ~120 nm (Figure 2b). To further stabilize the polymer assembly, light-induced dimerization of the coumarin moieties within the hydrophobic interior was used to crosslink the assembly's core. This dimerization-based crosslinking of the coumarin moieties was conveniently monitored by the decrease in the corresponding coumarin absorption peak (Figure 2c). The time-dependent nature of the decrease shows that the crosslink density of the assembly can be tuned, if necessary. The fact that the crosslinking process did not alter the size suggests that the morphology of the assembly is retained, which is further supported by transmission electron microscopy studies (Figure 2d,e).

Our design hypothesis is that the polymeric nanoassembly would not be able to bind to the target enzyme CA IX, until the ALP enzyme covalently cleaves the phosphate mask to reveal the sulfonamide ligands. To test this possibility, we used a competitive displacement assay, where 5-(dimethylamino)-1-naphthalenesulfonamide (DNSA) is used as the probe. The fluorescence signal of DNSA is higher when it is complexed to carbonic anhydrase and is much lower when is released into the aqueous phase.[9] Here, a CA-DNSA pre-complex would be fluorescent, but if the complexed DNSA is replaced by the surface sulfonamide ligand on the nanoassembly, its fluorescence at 460 nm would decrease significantly (Figure 3a).Since CA IX is a membrane protein, we used bovine carbonic anhydrase (bCA) as the surrogate protein for making the pre-complex. Our studies showed that when the ligands on the Nanoassemblies were

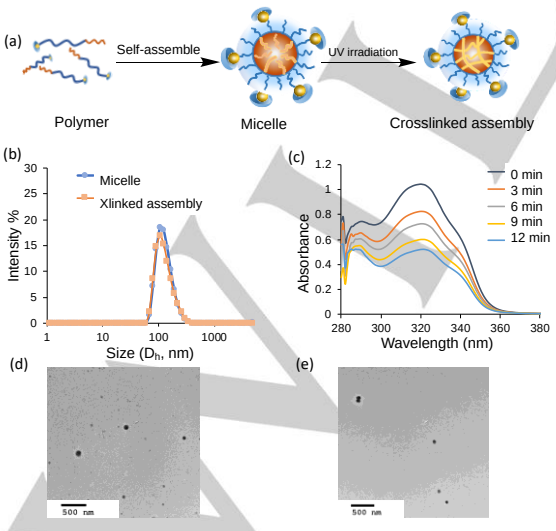

Figure 2. a) Preparation of crosslinked nanoassembly; b) DLS profile of micelle and crosslinked assembly; c) UV induced crosslinking of micelles; TEM images of (d) micelles and (e) crosslinked assembly.

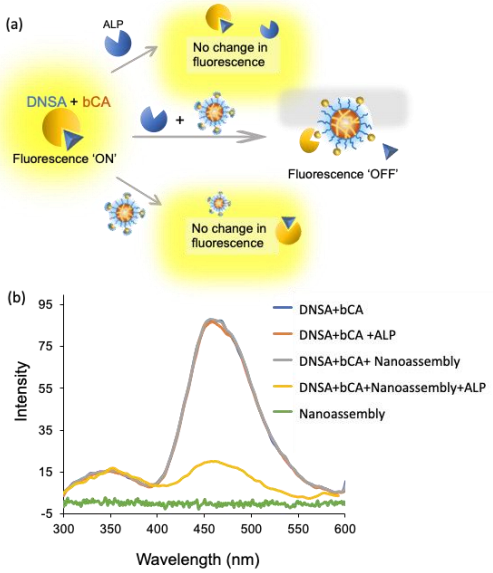

Figure 3. a) Scheme of DNSA-bCA competitive displacement assay, (b) Emission spectrum of DNSA-bCA complex when treated with Nanoassembly and ALP.

10.1002/anie.202002748

masked by the aryl phosphate moiety, it did not competitively remove DNSA, suggested by the little change of fluorescence intensity before and after the nanoassembly was added. However, when ALP was added to this system, significant fluorescent signal decrease was observed over 30 minutes, indicating that the unmasked ligand on the polymer nanoassembly surface was able to displace DNSA from the active site of bCA (Figure 3b). TEM images and DLS profile showed that morphology of nanoassemblies didn't change after ALP treatment (Figure S4, S5), zeta potential of particles increased from -23 mV to +2 mV, suggesting the cleavage of the phosphate mask (S5).

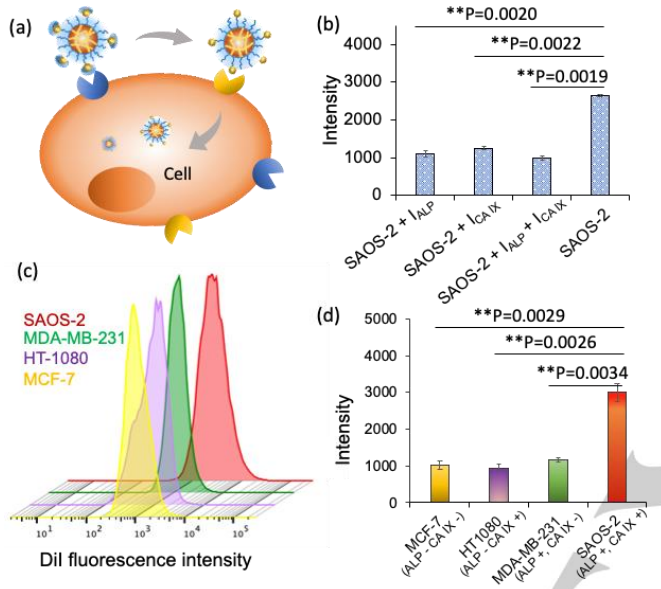

Figure 4. a) Schematic representation of 'Unicellular AND gate' b) Quantitative analysis of the fluorescence intensity of Cy3-labeled nanoparticles in SAOS-2 cells, c) Histograms of cellular uptake of DiI loaded nanogels in MCF-7, HT1080, MDA-MB-231 and SAOS-2 cells, d) Mean intensity of four cell lines showed the DiI loaded nanogel accumulation in four cell lines. Statistical significance was calculated via one-way ANOVA with a Tukey post-hoc test. *P < 0.05; **P < 0.01.

Following this confirmation, we were interested in testing the implications of this logic gate in cellular uptake (Figure 4a). SAOS-2 is a human osteosarcoma cell line that overexpresses both ALP and CA IX.35 Because of the presence of both these proteins on the same cell surface, this cell should serve to test the unicellular AND gate possibility, where the ALP processes the nanoassembly to reveal the sulfonamide ligand, which when recognized by the cell surface CA IX, will undergo an activated uptake inside the cells. To test this hypothesis, we loaded the polymeric assembly with a hydrophobic dye, 1,1'-dioctadecyl-3,3,3'3'-tetramethyl-indocarbocyanine perchlorate (DiI), to track and quantify the cellular uptake using flow cytometry and confocal laser scanning microscopy. We were excited to find that the accumulation of the assembly in Saos-2 cells is high (Figure S6). When treated Saos-2 cells with ALP pretreated Nanoassemblies, we observed a similar cellular uptake, suggesting ALP on the Saos-2 cells are sufficient to remove the phosphate mask and reveal the sulfonamide ligands (Figure S9). However, it is the comparison with appropriate controls that would clearly test if there is indeed an activated uptake based on the designed AND gate. To this end, we treated the Saos-2 cells with an ALP inhibitor or a CA IX inhibitor or the combination of the two, during the cellular uptake experiments. Indeed, the Saos-2 cells treated with either one or both of the inhibitors exhibited substantially lower cellular uptake, compared to the untreated cells (Figure 4b). These findings support our unicellular AND gate hypothesis that ALP and CA IX need to be concurrently present on the cell surface for the nanoassemblies to be taken up efficiently. These findings also confirm that the dye molecules are not passively diffusing into the cells.

To further investigate the unicellular AND gate possibility, we evaluated the selectivity of the nanoassemblies with four different cell lines. These cell lines were chosen for their variations in the levels of expression of ALP and CA IX on their surfaces, viz. Saos-2 (ALP+, CA IX+), MDA-MB-231 (ALP+, CA IX-), HT-1080 (ALP-, CA IX+) and MCF-7 (ALP-, CA IX-) cell lines. If the proposed unicellular AND gate pathway is operational, the accumulation of nanoassemblies will be only observed in the Saos-2 cells, where ALP and CA IX are concurrently overexpressed. The absence of either protein expression in other cell lines will suppress the accumulation of nanoassemblies. Indeed, DiI-loaded nanoassemblies are readily taken up by Saos-2 cells, but not by MDA-MB-231, HT-1080 or MCF-7 cells (Figure 4c,d).

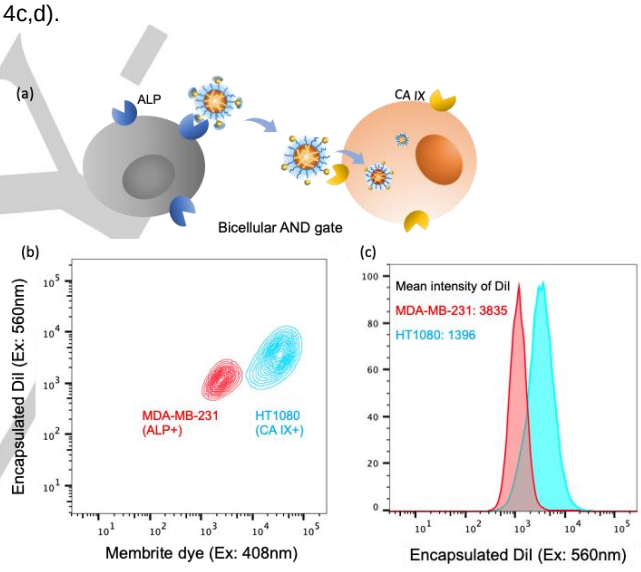

Figure 5. a) Schematic representation of 'Bicellular AND gate', b) Flow cytometry dual fluorescence density plot of HT1080 and MDA-MB-231 coculture (nanogel was loaded with DiI dye, HT1080 was stained with membrite dye), c) Histograms of nanogel uptake in HT1080 and MDA-MB-231 cells.

Unicellular AND gate operates when two different proteins are present on the same cell. Inspired by the cell-cell communication modalities seen in nature using two distinct proteins in two different cells, we were interested in investigating the possibility of bicellular AND gates in cellular uptake (Figure 5a). Here, the ALP on the surface of one cell would unmask the ligand moieties in the nanoassembly, while the CA IX on the surface of the second cell would cause active uptake. To test this idea, we cocultured two different cell lines, HT-1080 and MDA-MB-231, which overexpress CA IX and ALP on their surfaces respectively. The key here is the ability to differentiate the two cells in the microscope. For this purpose, HT1080 cells were stained with membrite dye (408 nm). DiI-loaded nanoassemblies were then added to the coculture and incubated for 1 hour. Although these

assemblies do not readily enter HT-1080 (CA IX+) cells or MDA-MB-231 (ALP+) cells when they were cultured separately, we observed a significant accumulation in HT-1080 (CA IX+) cells when they are cocultured with MDA-MB-231 (ALP+) (Figure 5b,c). These experiments show that the cell surface ALP in the latter cell line processes the nanogels to be taken up by the former cells after binding to the carbonic anhydrase.

In summary, we have demonstrated a set of cellular logic gates that exhibit efficient uptake of polymeric nanoassemblies in specific cells. The polymeric system contains a functional hydrophilic terminus based on a caged carbonic anhydrase-specific ligand, which can be unmasked with an ALP-catalyzed cleavage of an aryl phosphate group and a subsequent self-immolation reaction. Such a design offers to exhibit cellular AND gates in unicellular and bicellular settings. We show that these nanoassemblies are taken up efficiently and selectively by Saos-2 cells in single cell cultures, because this is the only cell line overexpresses both the unmasking enzyme ALP and the receptor protein CA IX, among the four cells tested. The same concept was then tested in a two-cell co-culture, where one cell overexpresses ALP (MDA-MB-231) and the other overexpresses CA IX (HT-1080). Here, only in the co-culture does the latter cell exhibits higher degree of uptake of the nanoassembly, because the former cell was able to unmask the ligand from the nanoassembly. The design insights and the concept of cellular AND gates provided here will find use in many applications where specificity in targeting is critical, because an AND-gate requires the concurrent presence of two different cell surface markers. Since proteins are arguably the most prominent pathological biomarkers, these dual protein-based cellular AND gate uptake of polymeric nanoassemblies would open up new possibilities for tumor imaging, diagnostics and targeted delivery.

Acknowledgements

We thank the National Science Foundation (CHE-1307118) for supporting this work. The microscopy data was gathered in the Light Microscopy Facility and Nikon Center of Excellence at the Institute for Applied Life Sciences, UMass Amherst with support from the Massachusetts Life Sciences Center. We thank Dr. Amy S. Burnside for help with Flow Cytometry data analysis.

Conflict of interest

The authors declare no conflict of interest.

Keywords: AND gate • Targeting • Cellular uptake • Enzyme-responsive polymeric nanoassembly

[1]. Mittelbrunn, M.; Sánchez-Madrid, F. *Nat. Rev. Mol. Cell Biol.* **2012**, 13, 328.

[2]. a) Seo, J.; Kim, S.; Park, H. H.; Choi, D. Y.; Nam, J. M. Nano- *Sci. Adv.* **2019**, *5*, 1–14. b) Callmann, C. E.; Barback, C. V.; Thompson, M. P.; Hall, D. J.; Mattrey, R. F.; Gianneschi, N. C. *Adv. Mater.* **2015**, *27*, 4611–4615. c) Long, M. J. C.; Poganik, J. R.; Aye, Y. *J. Am. Chem. Soc.* **2016**, *138* , 3610–3622. d) Wu, L.; Qu, X. *Chem. Soc. Rev.* **2015**, 44, 2963–2997. e) Liu, H. W.; Chen, L.; Xu, C.; Li, Z.; Zhang, H.; Zhang, X. B.; Tan, W. *Chem. Soc. Rev.* **2018**, 21, 7140–7180. f) Várady, G.; Cserepes, J.; Németh, A.; Szabó, E.; Sarkadi, B. *Biomark. Med.* **2013**, 7, 803–819. g) Shy, A. N.; Kim, B. J.; Xu, B. Matter **2019**, 1 , 1127–1147.

[3]. a) Maeda, H. *Adv. Drug Deliv. Rev*. **2015**, 91, 3–6. b) Battistella, C.; Callmann, C. E.; Thompson, M. P.; Yao, S.; Yeldandi, A. V.; Hayashi, T.; Carson, D. A.; Gianneschi, N. C. *Adv. Healthc. Mater.* **2019**, 1901105. c) Byrne, J. D.; Betancourt, T.; Brannon-Peppas, L. *Adv. Drug Deliv. Rev.* **2008**, 60, 1615–1626. d) Bae, Y. H.; Park, K. J. Control. release **2011**, 153, 198. e) Long, M. J. C.; Poganik, J. R.; Aye, Y. *J. Am. Chem. Soc.* 2**016**, 138, 3610–3622. f) A. B. Chinen, C. M. Guan, J. R. Ferrer, S. N. Barnaby, T. J. Merkel, C. A. Mirkin, *Chem. Rev.* **2015**, 115, 10530–10574. g) M. Elsabahy, G. S. Heo, S. Lim, G. Sun, K. L. Wooley, *Chem. Rev.* **2015**, 115, 10967−11011. h) A. R. Maity, D. Stepensky, Mol. Pharm. **2015**, 13, 1–7. i) M. W. Tibbitt, J. E. Dahlman, R. Langer, *J. Am. Chem. Soc.* **2016**, 138, 704−717.

[4]. a) Shi, J.; Xiao, Z.; Kamaly, N. Farokhzad, O.C. *Acc. Chem. Res.* **2011**, 44, 1123-1134. b) Cheng, Y.; Morshed, R.A.; Auffinger B.; Tobias, A.L. Lesniak, M.S. *Adv. Drug Deliv. Rev.* **2014**, 66, 42-57. c) Byrne, J.D.; Betancourt, T.; Brannon-Peppas, L. *Adv. Drug Deliv. Rev.* **2008**, 60, 1615-1626. d) Low, P.S. Henne W.A.; Doorneweerd, D.D., *Acc. Chem. Res.* **2008**, 41, 120-129. e) Feng, Z. Q. Q.; Wang, H. M.; Wang, S. Y.; Zhang, Q.; Zhang, X. X.; Rodal, A.; Xu, B. *J. Am. Chem. Soc.* **2018**, 140, 9566-9573

[5]. a) de Silva, A. P.; Uchiyama, S. *Nat. Nanotechnol.* **2007**, 399–410. b) Margulies, D.; Melman, G.; Felder, C. E.; Arad-Yellin, R.; Shanzer, A. *J. Am. Chem. Soc.* **2004**, 126, 15400–15401. c) Erbas-Cakmak, S.; Akkaya, E. U. *Angew. Chemie Int. Ed.* **2013**, 52, 11364–11368. d) De Silva, P. A.; Gunaratne, N. H. Q.; McCoy, C. P. *Nature* **1993**, 364, 42–44. e) Gao, J.; Liu, X.; Secinti, H.; Jiang, Z.; Munkhbat, O.; Xu, Y.; Guo, X.; Thayumanavan, S. *Chem. - A Eur. J.* **2018**, 24, 1789–1794.

[6]. a) Ellison, D.; Mugler, A.; Brennan, M. D.; Lee, S. H.; Huebner, R. J.; Shamir, E. R.; Woo, L. A.; Kim, J.; Amar, P.; Nemenman, I.; et al. *PNAS,* **2016**, 113, E679–E688. b) Lawrence, T. S.; Beers, W. H.; Gilula, N. B. *Nature* **1978**, 272, 501–506. c) Perbal, B. *Cell Commun Signal,* **2003**, 1, 3.

[7]. a) Rao, S. R.; Snaith, A. E.; Marino, D.; Cheng, X.; Lwin, S. T.; Orriss, I. R.; Hamdy, F. C.; Edwards, C. M. *Br. J. Cancer* **2017**, 116, 227–236. b) Fishman, W. H.; Inglis, N. R.; Green, S.; Anstiss, C. L.; Gosh, N. K.; Reif, A. E.; Rustigian, R.; Krant, M. J.; Stolbach, L. L. *Nature* **1968**, 219, 697,

[8]. Krishnamurthy, V. M.; Kaufman, G. K.; Urbach, A. R.; Gitlin, I.; Gudiksen, K. L.; Weibel, D. B.; Whitesides, G. M. *Chem. Rev.* **2008**, 108, 946–1051.

[9]. H. N. Li, Y. X. Ci, Anal. Chim. Acta **1995**, 317, 353–357.

10.1002/anie.202002748

Entry for the Table of Contents

Insert graphic for Table of Contents here.

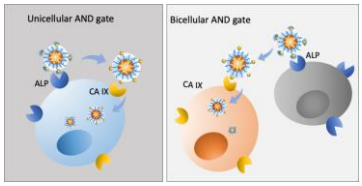

Insert text for Table of Contents here.

We showed here a set of cellular logic gates that exhibit efficient uptake of polymeric nanoassemblies in specific cell type, which were achieved by synergized effects of two different enzymes that are overexpressed on cell surface.